

PCCP

Accepted Manuscript



This is an *Accepted Manuscript*, which has been through the Royal Society of Chemistry peer review process and has been accepted for publication.

Accepted Manuscripts are published online shortly after acceptance, before technical editing, formatting and proof reading. Using this free service, authors can make their results available to the community, in citable form, before we publish the edited article. We will replace this *Accepted Manuscript* with the edited and formatted *Advance Article* as soon as it is available.

You can find more information about *Accepted Manuscripts* in the [Information for Authors](#).

Please note that technical editing may introduce minor changes to the text and/or graphics, which may alter content. The journal's standard [Terms & Conditions](#) and the [Ethical guidelines](#) still apply. In no event shall the Royal Society of Chemistry be held responsible for any errors or omissions in this *Accepted Manuscript* or any consequences arising from the use of any information it contains.

Selective Fluorescence Sensing of Polynitroaromatic Explosives by Triaminophenylbenzene Scaffolds

Cite this: DOI: 10.1039/x0xx00000x

Pratap Vishnoi, Mrinalini G. Walawalkar, Saumik Sen, Anindya Datta, G. Naresh Patwari, and Ramaswamy Murugavel*

Received 00th January 2012,
Accepted 00th January 2012

DOI: 10.1039/x0xx00000x

www.rsc.org/

Supramolecular fluorophore, 1,3,5-tris(4'-aminophenyl)benzene (TAPB) selectively senses polynitroaromatic compounds (PNAC), viz. 2,4,6-trinitrotoluene (TNT), 2,4-dinitrotoluene (DNT), picric acid (PA), *m*-dinitrobenzene (*m*-DNB) and *p*-dinitrobenzene (*p*-DNB) through donor-acceptor complexation. Steady-state and time resolved fluorescence measurements indicate predominantly static quenching of TAPB fluorophore with TNT, DNT, *m*-DNB and *p*-DNB. In the case of PA, a new emissive band with marginally longer lifetime emerges due to complex formation with TAPB. The selectivity of sensing action is rationalized through computation of HOMO and LUMO energies for both fluorophore and the analytes using M06-2X/6-311+G(d,p) level of theory. Practical utility of the fluorophore has also been demonstrated with TNT and DNT vapour.

1. Introduction

Given current security issues and threats, there is a critical need for on-field / on-site detection of explosives, particularly polynitroaromatic (PNAC) compounds such as 2,4,6-trinitrotoluene (TNT), 2,4-dinitrotoluene (DNT) and picric acid (PA).¹ Apart from conventional methods such as the use of canine teams,² and several sophisticated instrumental techniques viz X-ray scanning,³ ion mobility spectrometry (IMS),⁴ surface-enhanced Raman spectroscopy,⁵ gas chromatography coupled with mass spectrometry,⁶ and nuclear magnetic resonance spectroscopy⁷ are currently being employed for detection of PNAC. However, none of these techniques are ideal for on-field use because of their cost issues, bulkiness and susceptibility to false positives.⁸

Over the last decade, development of selective chemo-sensors has gained increased attention. Most of the available chemo-sensors utilize fluorescence detection due to its inherent sensitivity and cost-effectiveness. Change in fluorescence emission properties, such as quenching, enhancement and shift in the emission wavelength due to interaction of analytes with fluorophores can be used to develop functional fluorescent sensors.⁹ Low vapour pressure and limited chemical reactivity of PNAC make their detection challenging. However, their electron-deficient nature can be exploited to form stable donor-acceptor complexes with electron rich fluorophores, which can lead to fluorescence quenching via photoinduced electron transfer (PET) process.^{2b, 10-13}

To date, most fluorescent sensors for PNAC detection have been based on organic π -conjugated polymers (CPs)¹⁴ and more recently, metal-organic frameworks (MOFs),^{15, 16} oligo(*p*-phenylenevinylene) (OPV)-based gelators,¹⁷ and molecularly imprinted polymers (MIPs).¹⁸ The conjugated polymers based on pyrene, phenyleneethylene and phenylenevinylene have been known to offer appreciable sensitivity for nitrated

explosives through signal amplification, where the polymer backbone acts as a medium for long range exciton migration. Despite high sensitivity for the detection of explosives, the use of these polymeric materials is limited because of their complex synthetic methodologies. Therefore, a sensor with cost-effective synthesis and reusability is an ever increasing demand.

In an independent approach, small molecular fluorophores having rich π -donating character such as pyrene and anthracene present further opportunities for the detection strategies.¹⁹ An added advantage of these compounds is their easy synthesis and wider detection range for explosive compounds. It appears from some recent reports that the sensing efficiency and reusability of these discrete systems could be improved by substituting them with hydrogen bond active groups such as -COOH, -NH₂, -OH and others.^{10, 20} These groups extend the dimensionality of the small molecular systems to relatively stiff and extended network which could allow efficient analyte diffusion within the internal pores.²¹ Moreover, this will also lead to increase in the surface area of interaction between the host and the analyte, which can lead to efficient photophysical processes.

Considering these factors, photophysical properties and fluorescence based chemo-sensing of PNAC employing triphenylbenzene based C₃-symmetric systems are presented in this article. Triphenylbenzene systems are easily synthesizable inexpensive class of compounds and have widely been employed as building units in the synthesis of porous materials with moderate to high surface area.²² Despite having π -conjugation, their utility in luminescence based chemo-sensing applications is yet unexplored, possibly because of their non-planar (propeller shape) characteristics. Inspired by the hydrogen bonding assisted construction of organic and metallo-organic supramolecules reported by our group²³ in recent times and N-H...O bonding interactions of nitroanilines,²⁴ we have investigated the selective PNAC sensing capabilities of amino substituted triphenylbenzene, 1,3,5-tris(4'-aminophenyl)-

benzene (TAPB) both in solution and vapour phase. In addition to the formation of donor-acceptor π -interaction, amino groups can further interact through hydrogen bonding with the nitro groups of PNAC, leading to the enhanced sensing efficiency.

2. Experimental

2,4-Dinitrotoluene (Sigma-Aldrich), picric acid (Loba Chemie, India), *m*-dinitrobenzene (Thomas Baker, India) and *p*-dinitrobenzene (Specrochem, India), tetrafluorobenzene (Sigma-Aldrich), and hexafluorobenzene (Sigma-Aldrich) were procured from commercial sources and used after crystallization from suitable solvents. Methods used for purification of solvents are similar to those described in standard protocols.²⁵ 1,3,5-Tris(4'-aminophenyl)benzene (TAPB) was synthesized according to a published procedure.²⁶

Caution: Picric acid, TNT and DNT are sensitive to external stimuli such as shock, heat, electromagnetic radiation, static electricity etc. Although we did not face any kind of problem while working with them, it is highly advisable to handle these materials with due care.

2.1. Electronic spectroscopy

Absorption and emission spectra were recorded on Varian Cary Bio 100 UV-visible spectrophotometer and Varian Cary Eclipse fluorescence spectrometer, respectively. The absorption and emission spectra of TAPB were recorded in HPLC grade acetonitrile. Fluorescence emission spectra of TAPB solution were recorded by exciting at 290 nm. The TAPB fluorescence was titrated against the concentration of each PNAC analyte, which lead to fluorescence quenching. Similarly fluorescence quenching titrations were carried out for TAPB in the presence of hexafluorobenzene, 1,2,4,5-tetrafluorobenzene, benzonitrile and chlorobenzene. Time-resolved fluorescence decays were recorded using a time-correlated single-photon counting (TCSPC) system from IBH (UK). Time-resolved fluorescence decays were recorded with $\lambda_{\text{ex}} = 295$ nm and the emission polarizer set at a magic angle of 54.7° . The full width at half maximum (FWHM) of the instrument response function (IRF) is 700 ps and the resolution is 7 ps per channel. The data were fitted to single exponential function by the iterative re-convolution method using IBH DAS v6.2 data analysis software to obtain excited state lifetimes.²⁷

2.2. Vapour phase detection

A drop of acetonitrile solution (10^{-3} M) of TAPB was placed on a quartz plate and rotated on spin coater at 1000 rpm for two minutes to prepare a thin film. TNT (50 mg) was placed at the bottom of a quartz cuvette of 1 cm^2 cross-section and covered with a piece of cotton. The thin film was then inserted in the cuvette and the emission spectra were recorded with an interval of 2 minutes. The respective emission intensities were plotted as function of time to obtain quenching profile. Experiment was performed for DNT vapour in the same way.

2.3. Electrochemistry

The redox potential of TAPB (10^{-3} M) was determined by cyclic voltammetry (CV) in 0.1 M acetonitrile solution of *n*-Bu₄N(ClO₄) by using platinum disc electrode with a platinum wire auxiliary electrode and calomel as reference electrode. The experiments were performed on a CH Instruments, USA (Model; CHI1120A) with scan rate of 0.005 V/sec.

2.4. ¹H NMR titration

Proton NMR experiments were carried out on a Bruker 400 MHz instrument using DMSO-*d*₆ (D, 99.9%) as solvent. The chemical shift values are relative to the deuterated solvent peaks and are given in parts per million (ppm). 1.56 mL solution (8.57×10^{-2} M) of each TAPB and PA were prepared separately in DMSO-*d*₆. The TAPB solution was divided in 13 NMR tubes (labelled as a to k) as 0.24, 0.22, 0.20, 0.18, 0.16, 0.14, 0.12, 0.10, 0.08, 0.06, 0.04, 0.02 and 0.0 mL. The PA solution was added in such a way that the total volume in each tube remained constant at 0.24 mL. Each NMR sample was diluted to 0.28 mL by adding 0.04 mL of DMSO-*d*₆ before recording the NMR spectra. The spectra were recorded keeping machine parameters and temperature invariable. The change in chemical shifts, ($\Delta\delta$) of TAPB, were multiplied by corresponding values of mole fractions of TAPB (Δx) and plotted against mole fractions (Δx) to obtain the Job's plot.

2.6. Quantum chemical calculations

Unrestricted density functional theory calculations were carried out with Gaussian-09 (G09) suit of programs using GAUSSVIEW-5 graphical interface.²⁸ The M06-2X hybrid functional of Truhlar and Zhao²⁹ with 6-311+G(d,p) basis set for all atoms. The hybrid functional M06-2X has been widely used to compute non covalent interactions such as π -stacking.³⁰ To account for the influence of solvent (acetonitrile, $\epsilon = 35.688$), polarizable continuum model (PCM) calculations were performed utilizing self-consistent field approach in G09 using same level of theory.³¹ The geometries of TAPB and PNAC analytes (i.e. TNT, PA, *m*-DNB, *p*-DNB, DNT, and other analytes chlorobenzene, benzonitrile, tetrafluorobenzene, and hexafluorobenzene were optimized both in the gas phase and in the PCM.

3. Results and discussion

3.1. Fluorescence measurements

Free TAPB exhibits two prominent absorption bands (see Fig. S1) with peak maxima at 207 and 290 nm, attributed to π - π^* (S_0 - S_2) and n - π^* (S_0 - S_1) electronic transitions, respectively. TAPB showed a fluorescence emission at 405 nm when excited at 290 nm in an acetonitrile solution (see Fig. 1). Titration of TAPB with increasing concentration of PA leads to lowering of the emission intensity, as can be seen in Fig. 1. Titration of TAPB against other PNACs (TNT, DNT and *m*-DNB) also leads to fluorescence quenching (see Fig. 2a and S2-S5). The fluorescence quenching data were analysed using Stern-Volmer equation.

$$\frac{I_0}{I} = 1 + K_{SV}[Q]$$

where I_0 is the initial emission intensity of TAPB prior to addition of quencher, I is the emission intensity at any given concentration $[Q]$ of the quencher and K_{SV} is the Stern-Volmer constant.³² In all the four cases near-linear Stern-Volmer plots (Fig. 2b) were obtained in the lower quencher (PNAC) concentrations, which indicate a single quenching mechanism.³³ The Stern-Volmer constants for all the analytes are listed in Table 1.

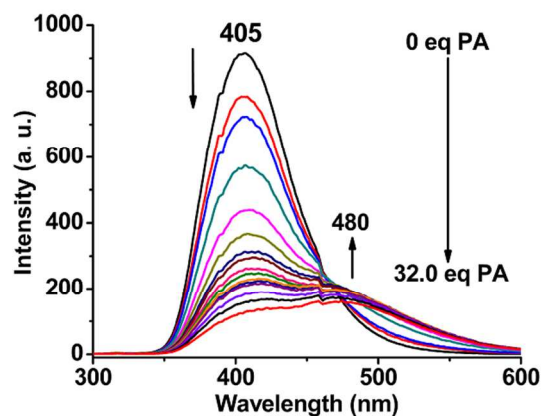


Fig. 1 Fluorescence quenching profile of TAPB (1.0 μM) in acetonitrile) with PA (0-32 eq).

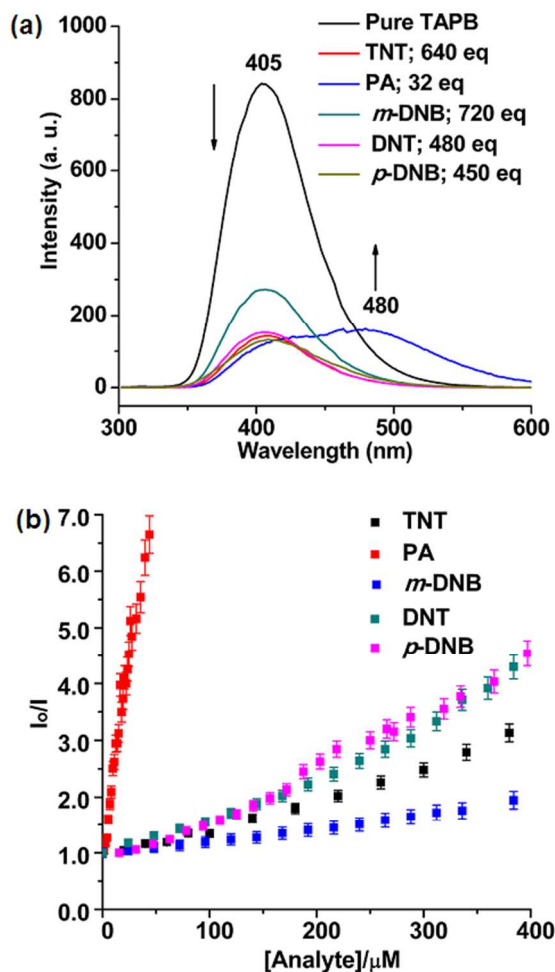


Fig. 2 (a) Combined fluorescence quenching profile of TAPB (1.0 μM in acetonitrile) with TNT (640 eq), PA (32 eq), *m*-DNB (720 eq), DNT (480 eq) and *p*-DNB (450 eq) and (b) Corresponding Stern-Volmer plots.

It can be seen from Fig. 2a that PA is much more efficiently quenches the fluorescence of TAPB (85% quenching upon

Table 1 Details of quenching efficiencies for TAPB with PNAC analytes.

Analyte(s)	Eq added	% Quenching	K_{sv} (M^{-1})
PA	32	85	1.2×10^5
TNT	640	82	4.0×10^3
<i>m</i> -DNB	720	67	2.6×10^3
DNT	480	82	8.3×10^3
<i>p</i> -DNB	450	85	8.0×10^3

addition of 32.0 equivalents) in comparison to other four PNAC analytes. Although PA and other PNAC analytes have similar reduction potentials (E_{red} for PA = -0.65,³⁴ for TNT = -0.7, for DNT = -1.0, for *m*-DNB = -0.9 V and for *p*-DNB = -0.7 V) (vs SCH).³⁵ The high quenching efficiency of PA may be rationalized in terms of high electron-deficiency of PA³⁶ coupled with the proton transfer from acidic -OH to -NH₂ group of TAPB (formation of -NH₃⁺ on TAPB). The new emission band at around 480 nm (see Fig. 1 and 2a) is because of the emissive nature of the TAPB-PA complex. The relative fluorescence quenching efficiency of various PNAC analytes is summarized in the bar diagram in Fig. 3.

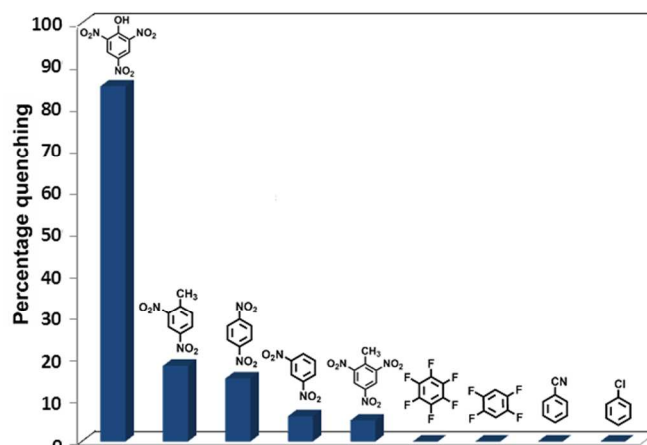


Fig. 3 Comparison of fluorescence quenching of TAPB observed in acetonitrile solvent after addition of 32.0 eq of each PNAC and other analytes.

3.2. Time resolved fluorescence measurements

The Stern-Volmer constant provides the information about the efficiency of quenching with little insight into the mechanism involved in quenching process. The apparent linearity of the Stern-Volmer plots at low concentration indicated that the processes are governed mainly by a single mechanism. To elucidate the fact, viz. whether the quenching occurred by ground state binding of quencher molecules with the fluorophore and forming a non-emissive species (static quenching) or a fast collision between them in excited state (dynamic quenching), the excited state lifetimes and fluorescence decays were measured before and after multiple additions of nitrated analytes.

TAPB exhibits a single exponential decay at emission wavelength of 405 nm with lifetime of 6.3 ns (see Fig. 4). For TAPB-PA complex, the lifetime at 405 nm remains constant at

ca. 6.3 ns, indicating static quenching. The lifetime at 480 nm also remains constant at ca. 9.2 ns, indicating the formation of a new emissive species with a longer lifetime as a result of the complexation. For the other four analytes, the lifetime of the 405 nm band decreases very gradually indicating the nature of quenching is predominately static (see Fig. S6). The details of lifetimes of excited states and corresponding fitting parameters have been given in the Table 2.

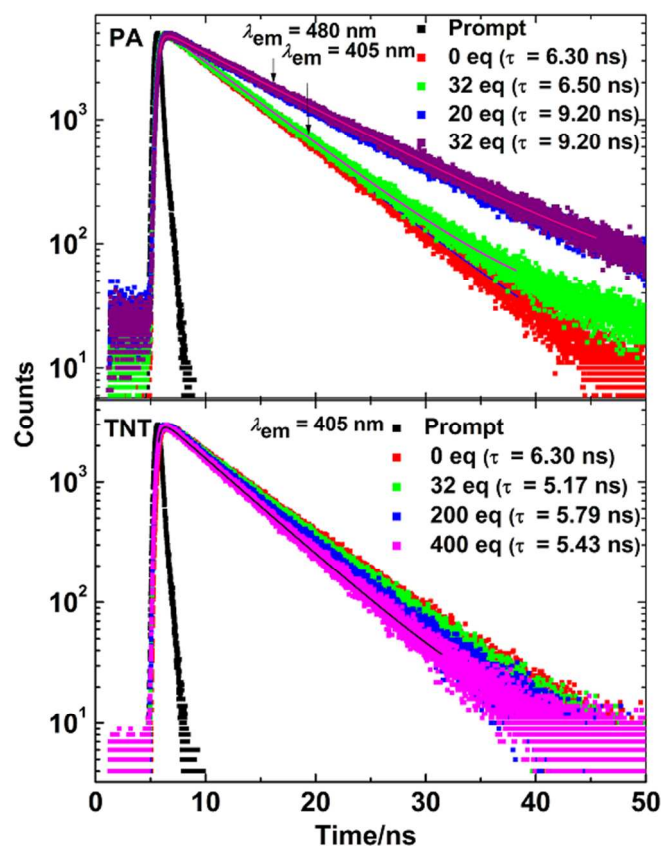


Fig. 4 Time resolved fluorescence decays for acetonitrile solution of TAPB before and after multiple additions of known concentrations of PA, TNT, *m*-DNB, DNT and *p*-DNB. Single exponential fits to the decays are included as solid lines.

3.3. Selectivity

Fluorescence measurements of TAPB carried out in the presence of other electron deficient species such as hexafluorobenzene, 1,2,4,5-tetrafluorobenzene, benzonitrile and chlorobenzene clearly establish that these four molecule do not quench the fluorescence. These results signify that the sensitivity and selectivity of quenching of TAPB fluorescence by PNAC (Figures S7-S10). An explanation for this selectivity is sought through quantum chemical computations. In the case of complexes formed between electron-rich and electron-deficient species, photoinduced electron transfer (PET) is the dominant quenching mechanism. The frontier orbital diagram for such a mechanism is schematically shown in Fig. 5.

The computed HOMO and LUMO energies for TAPB along with PNAC and other electron-deficient molecules are shown in Fig. 6, which clearly indicates the feasibility of PET selectively from

TAPB to the PNAC. On the other hand, it can be seen that the LUMOs of hexafluorobenzene, 1,2,4,5-tetrafluorobenzene, benzonitrile and chlorobenzene, and the LUMO of TAPB (fluorophore) are almost at the same energy, which renders the PET process unfavourable.

Table 2 The details of lifetimes of excited states and corresponding fitting parameters at $\lambda_{em} = 405$ nm of TAPB.

Analyte(s)	Eq(s) added	Lifetime (τ)/ns	χ^2
-	-	6.29	1.00
PA	32	6.50	1.07
TNT	32	6.17	1.04
	200	5.79	1.00
	400	5.43	1.00
DNT	32	6.12	1.04
	200	5.83	1.04
	400	5.49	1.02
<i>m</i> -DNB	32	6.20	1.00
	200	5.91	1.02
	400	5.56	1.05
<i>p</i> -DNB	32	6.16	1.00
	200	5.91	1.04
	400	5.65	1.04

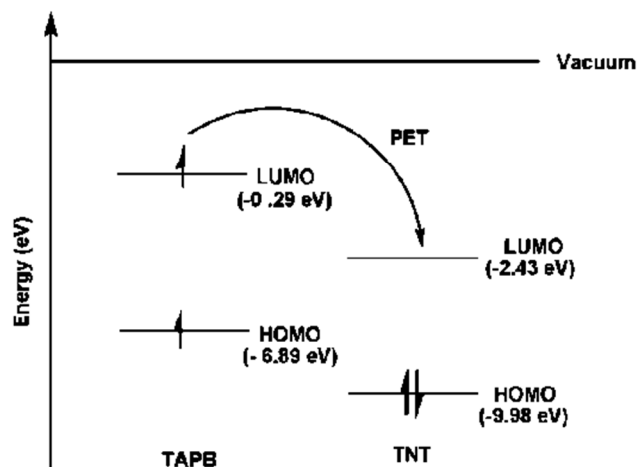


Fig. 5 Mechanism of photoinduced electron transfer from fluorophore to quencher (TNT).

3.4. Vapour phase fluorescence quenching studies

To demonstrate the utility towards vapour phase detection of PNAC, thin films of TAPB are spin coated on a quartz plate. The fluorescence spectra of the thin films have been recorded in the presence of TNT and DNT vapour as a function of time. The extent of fluorescence quenching increases progressively with exposure time (see Fig. 7). TAPB film lost nearly 60% of the fluorescence

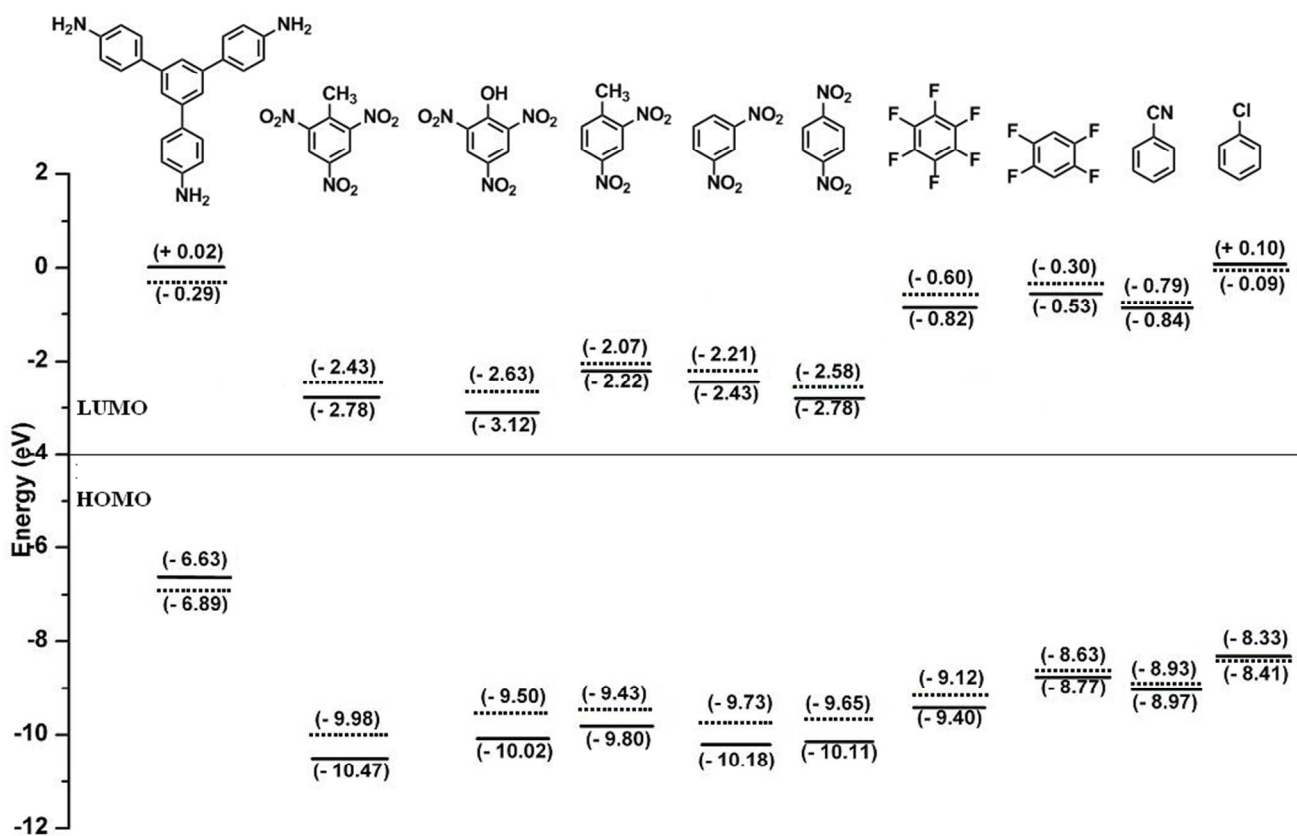


Fig. 6 Energy correlation diagram of the frontier orbitals of fluorophore, quenchers and other electronegative analytes in gas phase (solid lines) and in acetonitrile (dotted lines).

To demonstrate the utility towards vapour phase detection of PNAC, thin films of TAPB are spin coated on a quartz plate. The fluorescence spectra of the thin films have been recorded in the presence of TNT and DNT vapour as a function of time. The extent of fluorescence quenching increases progressively with exposure time (see Fig. 7). TAPB film lost nearly 60% of the fluorescence

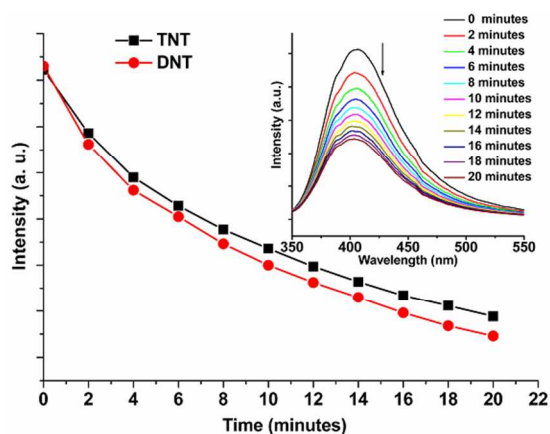


Fig. 7 Quenching efficiency curves of TAPB thin film upon exposure to vapours of TNT and DNT against time. The inset shows quenching profile of TAPB thin film with TNT vapour.

3.5. Determination of stoichiometry in the solution phase

Binding stoichiometry of TAPB with PNAC in solution has been determined by using Benesi–Hildebrand equation (see Fig. 8).³⁷

$$\frac{1}{I - I_0} = \frac{1}{I_1 - I_0} + \frac{1}{K_a(I_1 - I_0)[Q]}$$

where I_0 is the intensity of fluorescence before addition of the quencher, I is the intensity of emission at any given concentration of the quencher, I_1 is the intensity upon saturation with the quencher, K_a is the association constant and $[Q]$ is the concentration of the quencher.

The observed linear fits with TNT, *m*-DNB, *p*-DNB and DNT indicate 1:1 binding stoichiometry. With picric acid, however, a 1:2 complex is formed which yields a linear fit to the modified Benesi–Hildebrand equation

$$\frac{1}{I - I_0} = \frac{1}{I_1 - I_0} + \frac{1}{K_a(I_1 - I_0)[PA]^2}$$

The stoichiometry of TAPB-PA complex is further confirmed by Job's method of continuous variation monitoring chemical shifts in the ¹H NMR spectra of TAPB (see Fig. 9). The spectral analysis

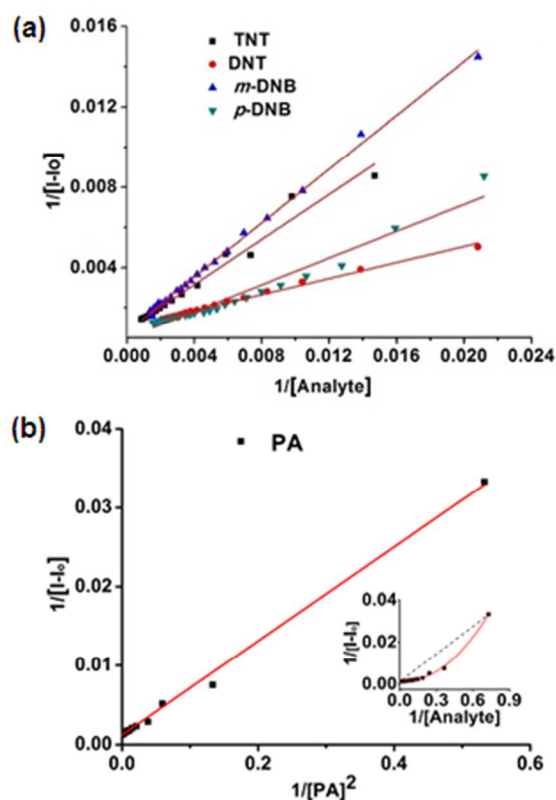


Fig. 8 Benesi-Hildebrand plots of TAPB (1.0 μM in acetonitrile) with (a) TNT, *m*-DNB, DNT and *p*-DNB, and (b) PA, where inset shows the curve assuming 1:1 complex formation.

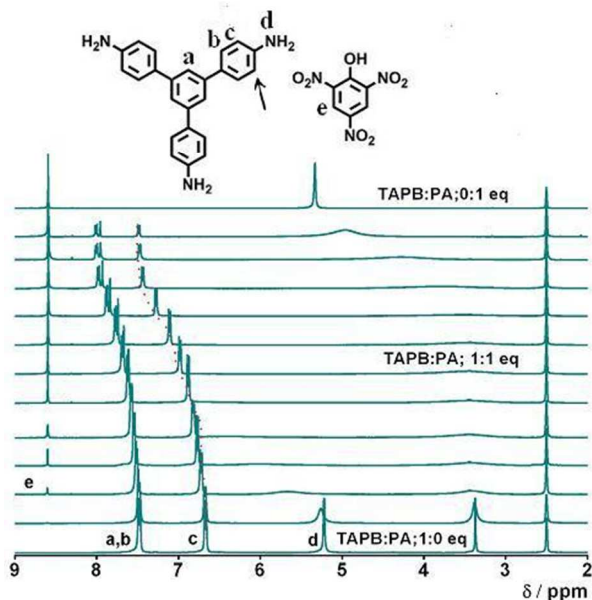


Fig. 9 ^1H NMR spectra for Job's plot of TAPB-PA system in $\text{DMSO-}d_6$. The peak labelled as *c* is considered for the calculations.

suggested the presence of PA caused significant downfield shifts of the aromatic protons of TAPB. The peak maximum in Job's plot at 0.36 indicated the formation of 1:2 complex (see Fig. S11).

3.6. Cyclic voltammetry of TAPB

Cyclic voltammogram of TAPB exhibits three irreversible oxidation stages, assigned to the successive oxidation of three $-\text{NH}_2$ groups (see Fig. 10). Oxidation potentials of these peaks as calculated from the cyclic voltammogram are 0.68, 1.10 and 1.65 V with respect to standard calomel electrode.

In contrast, PNAC compounds show negative (cathodic) peak potentials (see above) which indicates their facile reduction and electron acceptor character. In other word, these analytes can easily accept the electron from TAPB to form donor-acceptor complexes.

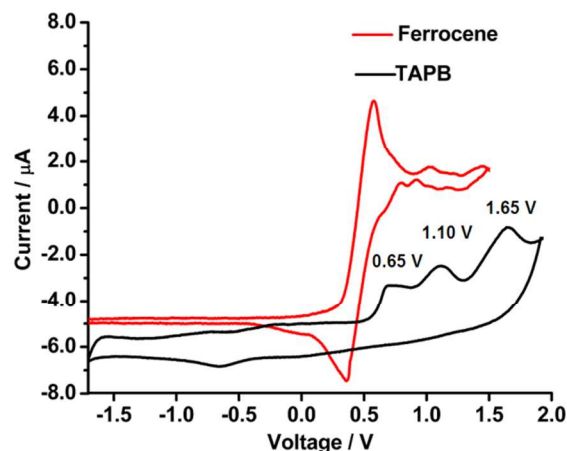


Fig. 10 Cyclic voltammogram of (a) TAPB and (b) ferrocene.

4. Conclusion

1,3,5-Tris(4'-aminophenyl)benzene is a supramolecular fluorescent sensor for polynitroaromatic compounds such as TNT, DNT and PA which are major constituent of the most explosives. These nitro compounds quench the emission intensity of the fluorophore of TAPB both in solution and vapour phase due to selective and strong donor-acceptor binding which has been further rationalized through frontier orbital calculations.

We believe that the results presented in this investigation not only provide a new way for rapid fluorescence detection of PNAC but also opens up possibilities of using such electron-rich π -conjugated discrete molecules in the development of effective chemo-sensory materials for selective detection of nitroaromatic explosives.

Notes

Department of Chemistry,
Indian Institute of Technology Bombay, Mumbai, India-400 076
E-mail; rmv@chem.iitb.ac.in

Acknowledgements

We thank Department of Science and Technology, New Delhi and Department of Atomic Energy, Mumbai, India for financial support. P. V. and S. S. thank CSIR for research fellowship (SRF). We are also thankful to Prof. Anil Kumar for extending some of his lab facilities.

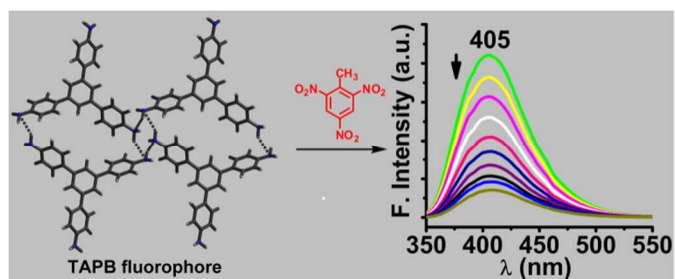
Supporting information

Cyclic voltammogram, additional UV-Vis and fluorescence spectra. See DOI: 10.1039/b000000x/

References

- (1) (a) K. D. Smith, B. R. McCord, W. A. McCrehan, K. Mount and W. F. Rowe, *J. Forensic Sci.*, 1999, **44**, 789-794. (b) G. R. Lotufo, J. D. Farrar, L. S. Inouye, T. S. Bridges and D. B. Ringelberg, *Environ. Toxicol. Chem.*, 2001, **20**, 1762-1771.
- (2) (a) A. W. Czarnik, *Nature*, 1998, **394**, 417-418. (b) T. Caron, M. Guillemot, P. Montméat, F. Veignal, F. Perraut, P. Prené and F. Serein-Spirau, *Talanta*, 2010, **81**, 543-548.
- (3) S. F. Hallowell, *Talanta*, 2001, **54**, 447-458.
- (4) (a) R. G. Ewing and C. J. Miller, *Field Anal. Chem. Technol.*, 2001, **5**, 215-221. (b) S. W. Thomas, J. P. Amara, R. E. Bjork and T. M. Swager, *Chem. Commun.*, 2005, 4572-4574.
- (5) J. M. Sylvia, J. A. Janni, J. D. Klein, and K. M. Spencer, *Anal. Chem.*, 2000, **72**, 5834-5840.
- (6) K. Håkansson, R. V. Coorey, R. A. Zubarev, V. L. Talrose and P. J. Håkansson, *Mass Spectrom.*, 2000, **35**, 337-346.
- (7) S. R. Wallenborg and C. G. Bailey, *Anal. Chem.*, 2000, **72**, 1872-1878.
- (8) (a) Y. Salinas, R. Martinez-Manez, M. D. Marcos, F. Sancenon, A. M. Costero, M. Parra and S. Gil, *Chem. Soc. Rev.*, 2012, **41**, 1261-1296. (b) M. S. Meaney and V. L. McGuffin, *Anal. Chim. Acta*, 2008, **610**, 57-67.
- (9) (a) J. V. Goodpaster and V. L. McGuffin, *Anal. Chem.*, 2001, **73**, 2004-2011. (b) T. M. Swager, *Acc. Chem. Res.*, 1998, **31**, 201-207. (c) S. Singh, *J. Hazard. Mater.*, 2007, **144**, 15-28. (d) J. Li, C. E. Kendig and E. E. Nesterov, *J. Am. Chem. Soc.*, 2007, **129**, 15911-15918. (e) S. M. Fonseca, R. P. Galvão, H. D. Burrows, A. Gutacker, U. Scherf and G. C. Bazan, *Macromol. Rapid Commun.*, 2013, **34**, 717-722.
- (10) S. Shanmugaraju, H. Jadhav, R. Karthik and P. S. Mukherjee, *RSC Advances*, 2013, **3**, 4940-4950.
- (11) A. Vu, J. Phillips, P. Bühlmann and A. Stein, *Chem. Mater.*, 2013, **25**, 711-722.
- (12) J. C. Sanchez, A. G. DiPasquale, A. L. Rheingold and W. C. Trogler, *Chem. Mater.*, 2007, **19**, 6459-6470.
- (13) W. Wei, X. Huang, K. Chen, Y. Tao and X. Tang, *RSC Advances*, 2012, **2**, 3765-3771.
- (14) (a) S. W. Thomas, G. D. Joly and T. M. Swager, *Chem. Rev.*, 2007, **107**, 1339-1386. (b) S. J. Toal and W. C. Trogler, *J. Mater. Chem.*, 2006, **16**, 2871-2883. (c) J.-S. Yang and T. M. Swager, *J. Am. Chem. Soc.*, 1998, **120**, 5321-5322.
- (15) (a) P. Kolla, *Angew. Chem., Int. Ed.*, 1997, **36**, 800-811. (b) B. Gole, A. K. Bar, and P. S. Mukherjee, *Chem. Commun.*, 2011, **47**, 12137-12139. (c) C. Zhang, Y. Che, Z. Zhang, X. Yang, and L. Zang, *Chem. Commun.*, 2011, **47**, 2336-2338. (d) S. Pramanik, C. Zheng, X. Zhang, T. J. Emge and J. Li, *J. Am. Chem. Soc.*, 2011, **133**, 4153-4155. (e) Zhang, Z. S. Xiang, X. Rao, Q. Zheng, F. R. Fronczek, B. Qian and G. Chen, *Chem. Commun.*, 2010, **46**, 7205-7207.
- (16) (a) A. K. Chaudhari, S. S. B. Nagarkar, Joarder and S. K. Ghosh, *Cryst. Growth Des.*, 2013, **13**, 3716-3721. (b) S. S. Nagarkar, B. Joarder, A. K. Chaudhari, S. Mukherjee and S. K. Ghosh, *Angew. Chem., Int. Ed.*, 2013, **52**, 2881-2885.
- (17) K. K. Kartha, S. S. Babu, S. Srinivasan and A. Ajayaghosh, *J. Am. Chem. Soc.*, 2012, **134**, 4834-4841.
- (18) (a) T.-P. Huynh, M. Sosnowska, J. W. Sobczak, C. B. Kc, V. N. Nesterov, F. D'Souza and W. Kutner, *Anal. Chem.*, 2013, **85**, 8361-8368. (b) A. Pietrzyk, S. Suriyanarayanan, W. Kutner, R. Chitta and F. D'Souza, *Anal. Chem.*, 2009, **81**, 2633-2643. (c) R. Chitta, A. S. D. Sandanayaka, A. L. Schumacher, L. D'Souza, Y. Araki, O. Ito and F. D'Souza, *J. Phys. Chem. C*, 2007, **111**, 6947-6955.
- (19) M. E. Germain and M. J. Knapp, *Chem. Soc. Rev.*, 2009, **38**, 2543-2555.
- (20) B. Gole, S. Shanmugaraju, A. K. Bar and P. S. Mukherjee, *Chem. Commun.*, 2011, **47**, 10046-10048.
- (21) N. Venkatramaiah, S. Kumar and S. Patil, *Chem. Commun.*, 2012, **48**, 5007-5009.
- (22) (a) P. Kuhn, M. Antonietti and A. Thomas, *Angew. Chem., Int. Ed.*, 2008, **47**, 3450-3453. (b) Z. Wang, B. Zhang, H. Yu, G. Li and Y. Bao, *Soft Matter.*, 2011, **7**, 5723-5730. (c) F. J. Uribe-Romo, C. J. Doonan, H. Furukawa, K. Oisaki and O. M. Yaghi, *J. Am. Chem. Soc.*, 2011, **133**, 11478-11481. (d) A. P. Cote, H. M. El-Kaderi, H. Furukawa, J. R. Hunt and O. M. Yaghi, *J. Am. Chem. Soc.*, 2007, **129**, 12914-12915. (e) H. Li, M. Eddaoudi, M. O'Keeffe and O. M. Yaghi, *Nature*, 1999, **402**, 276-279.
- (23) (a) R. Murugavel, S. Kuppaswamy, R. Boomishankar and A. Steiner, *Angew. Chem., Int. Ed.*, 2006, **45**, 5536-5540. (b) S. Banerjee and R. Murugavel, *Cryst. Growth Des.*, 2004, **4**, 545-552. (c) R. Murugavel, R. Pothiraja, S. Shanmugan, N. Singh and R. J. Butcher, *J. Organomet. Chem.*, 2007, **692**, 1920-1923. (d) R. Murugavel and S. Shanmugan, *Chem. Commun.*, 2007, 1257-1259. (e) R. Murugavel, and S. Banerjee, *Inorg. Chem. Commun.*, 2003, **6**, 810-814. (f) R. Murugavel, V. V. Karambelkar, G. Anantharaman and M. G. Walawalkar, *Inorg. Chem.*, 2000, **39**, 1381-1390.
- (24) T. W. Panunto, Z. Urbanczyk-Lipkowska, R. Johnson and M. C. Etter, *J. Am. Chem. Soc.*, 1987, **109**, 7786-7797.
- (25) Purification of Laboratory Chemicals, D. D. Perrin, Armarego W.L.F.; Pergamon Press; 3rd Ed. 1988.
- (26) C. Bao, R. Lu, M. Jin, P. Xue, C. Tan, T. Xu, G. Liu and Y. Zhao, *Chem. Eur. J.*, 2006, **12**, 3287-3294.
- (27) T. K. Mukherjee and A. Datta, *J. Phys. Chem. B*, 2006, **110**, 2611-2617.
- (28) Frisch, M. J. *et al. Gaussian, Inc.*, Wallingford CT, 2009.
- (29) Y. Zhao, and D. G. Truhlar, *Theor. Chem. Acc.*, 2008, **120**, 215-241.
- (30) (a) Y. Zhao and D. G. Truhlar, *Acc. Chem. Res.*, 2008, **41**, 157-167. (b) R. Valero, R. Costa, I. de P. R. Moreira, D. G. Truhlar and F. Illas, *J. Chem. Phys.*, 2008, **128**, 114103-114108. (c) V. S. Bryantsev, M. S. Diallo, A. C. T. van Duin and W. A. Goddard III, *J. Chem. Theory Comput.*, 2009, **5**, 1016-1026. (d) D. Jacquemin, E. A. Perpete, I. Ciofini, C. Adamo, R. Valero, Y. Zhao and D. G. Truhlar, *J. Chem. Theory Comput.*, 2010, **6**, 2071-2085.
- (31) (a) J. Tomasi, B. Mennucci and R. Cammi, *Chem. Rev.*, 2005, **105**, 2999-3093. (b) J. Tomasi, B. Mennucci and E. Cancès, *J. Mol. Struct. (Theochem)*, 1999, **464**, 211-226. (c) J. Tomasi, R. Cammi, B. Mennucci, C. Cappelli and S. Corni, *Phys. Chem. Chem. Phys.*, 2002, **4**, 5697-5712.
- (32) J. Lackowicz, *Principles of Fluorescence Spectroscopy*; Plenum Press: New York, 1983.
- (33) T. K. Mukherjee, P. P. Mishra and A. Datta, *Chem. Phys. Lett.*, 2005, **407**, 119-123.
- (34) J.-S. Yang and T. M. Swager, *J. Am. Chem. Soc.*, 1998, **120**, 11864-11873-11873.
- (35) I. Bergman and J. C. James, *Trans. Faraday Soc.*, 1954, **50**, 60-65.
- (36) (a) S. Ghosh and P. S. Mukherjee, *Organometallics*, 2008, **27**, 316-319. (b) S. Ghosh, B. Gole, A. K. Bar and P. S. Mukherjee, *Organometallics*, 2009, **28**, 4288-4296.
- (37) (a) H. A. Benesi and J. H. Hildebrand, *J. Am. Chem. Soc.*, 1949, **71**, 2703-2707. (b) P. P. Mishra, A. L. Koner and A. Datta, *Chem. Phys. Lett.*, 2004, **400**, 128-132.

Table of content



C₃-symmetric 1,3,5-Tris(4'-aminophenyl)benzene has been employed as a selective fluorescence chemo-sensor for polynitroaromatic compounds.